


ORIGINAL ARTICLE

Intraperitoneal administration of nanoparticles containing tocopheryl succinate prevents peritoneal dissemination

Susumu Hama¹  | Takayuki Nishi² | Eitaro Isono¹ | Shoko Itakura³ |
Yutaka Yoshikawa⁴ | Akinori Nishimoto² | Satoko Suzuki² | Naoko Kirimura² |
Hiroaki Todo³ | Kentaro Kogure⁵

¹Faculty of Pharmacy, Research Institute of Pharmaceutical Sciences, Musashino University, Tokyo, Japan

²Department of Biophysical Chemistry, Kyoto Pharmaceutical University, Kyoto, Japan

³Faculty of Pharmacy and Pharmaceutical Sciences, Josai University, Saitama

⁴Department of Health, Sports, and Nutrition, Faculty of Health and Welfare, Kobe Women's University, Kobe, Japan

⁵Institute of Biomedical Sciences, Tokushima University Graduate School, Tokushima, Japan

Correspondence

Susumu Hama, Research Institute of Pharmaceutical Sciences, Faculty of Pharmacy, Musashino University, 1-1-20 Shinmachi Nishitokyo-shi, Tokyo, 202-8585, Japan.
Email: s-hama@musashino-u.ac.jp

Funding information

JSPS KAKENHI, Grant/Award Number: 18H03540

Abstract

Intraperitoneal administration of anticancer nanoparticles is a rational strategy for preventing peritoneal dissemination of colon cancer due to the prolonged retention of nanoparticles in the abdominal cavity. However, instability of nanoparticles in body fluids causes inefficient retention, reducing its anticancer effects. We have previously developed anticancer nanoparticles containing tocopheryl succinate, which showed high *in vivo* stability and multifunctional anticancer effects. In the present study, we have demonstrated that peritoneal dissemination derived from colon cancer was prevented by intraperitoneal administration of tocopheryl succinate nanoparticles. The biodistribution of tocopheryl succinate nanoparticles was evaluated using inductively coupled plasma mass spectroscopy and imaging analysis in mice administered quantum dot encapsulated tocopheryl succinate nanoparticles. Intraperitoneal administration of tocopheryl succinate nanoparticles showed longer retention in the abdominal cavity than by its intravenous (i.v.) administration. Moreover, due to effective biodistribution, tumor growth was prevented by intraperitoneal administration of tocopheryl succinate nanoparticles. Furthermore, the anticancer effect was attributed to the inhibition of cancer cell proliferation and improvement of the intraperitoneal microenvironment, such as decrease in the levels of vascular endothelial growth factor A, interleukin 10, and M2-like phenotype of tumor-associated macrophages. Collectively, intraperitoneal administration of tocopheryl succinate nanoparticles is expected to have multifaceted antitumor effects against colon cancer with peritoneal dissemination.

KEYWORDS

ascites, intraperitoneal administration, nanoparticles, peritoneal dissemination, tocopheryl succinate

Abbreviations: colon26-Luc, colon26 cells stably expressing the luciferase gene; DOTAP, 1,2-dioleoyl-3-trimethylammonium propane; EPC, egg phosphatidylcholine; IL-10, interleukin 10; PDI, polydispersity index; Qd, quantum dots; R8-Qd, carboxyl-Qd modified with STR-R8; Rh-PE, 1,2-dioleoyl-sn-glycero-3-phosphoethanolamine-N-(lissamine rhodamine B sulfonyl); STR-R8, stearylated octaarginine; TAM, tumor-associated macrophages; TNF- α , tumor necrosis factor alpha; TS, α -Tocopheryl succinate; TS-NP, tocopheryl succinate nanoparticles; TS-NP-Qd, Qd encapsulated in TS-NP; VEGF-A, vascular endothelial growth factor A; α -T, α -tocopherol.

This is an open access article under the terms of the [Creative Commons Attribution-NonCommercial](https://creativecommons.org/licenses/by-nc/4.0/) License, which permits use, distribution and reproduction in any medium, provided the original work is properly cited and is not used for commercial purposes.

© 2022 The Authors. *Cancer Science* published by John Wiley & Sons Australia, Ltd on behalf of Japanese Cancer Association.

1 | INTRODUCTION

During the development of rational cancer therapy, nanoparticles such as liposomes, micelles, and lipid nanoparticles have been used for the delivery of hydrophobic and hydrophilic drugs and nucleic acids.¹⁻³ Tumor site-specific delivery along with improvement in solubility and avoidance of enzymatic degradation of various drugs can be achieved through nanoparticle formulations.⁴⁻⁶ When nanoparticles are intravenously (i.v.) administered, they are passively delivered to tumor tissues via the enhanced permeability and retention (EPR) effect.⁷ However, this delivery strategy using EPR effect requires the high circulation of nanoparticles in the blood and a specific physiological environment within the tumor, particularly hypervascularity.⁸ Therefore, it is difficult to deliver nanoparticles to pancreatic cancer or peritoneal dissemination with hypovascularity by i.v. administration, even if the nanoparticles show excellent blood circulation.⁹⁻¹¹

Peritoneal dissemination is a major cause of death in abdominal cancers such as colon and gastric cancers rather than the peritoneal cancer itself.^{12,13} During cancer progression, the cells disseminate into the peritoneal cavity and then metastasize to the peritoneum.^{12,13} Therefore, chemotherapy is needed to prevent further spread of cancer cells in the peritoneum and peritoneal cavity, in addition to killing cancer cells directly. Alternatively, extensive formation of ascites occurs in an abnormal peritoneum, leading to decrease in the quality of life of patients.¹⁴ In the potential mechanism underlying the formation of ascites it is considered that the leaky structure of tumor vessels alters the direction of oncotic pressure, leading to the flow of ascites into the peritoneal cavity.^{15,16} A rational strategy to prevent the formation of ascites is to stabilize the vascular structure in addition to killing cancer cells.

Systemic administration of anticancer drugs via the i.v. route for the treatment of peritoneal dissemination is inefficient for achieving therapeutic efficacy due to the inferior transitivity of drugs into the peritoneum and peritoneal cavity.^{17,18} To improve drug transitivity, intraperitoneal (i.p.) administration of anticancer drugs has a focus of study.^{17,18} Anticancer drugs administered via the i.p. route can directly attack cancer cells in the peritoneum and peritoneal cavity at a high local concentration.^{19,20} Furthermore, the i.p. retention time of drugs is affected by the size of the drug. Large-sized drug formulations such as anticancer nanoparticles remain in the peritoneal cavity for a long duration, while small-sized drug formulations enter the systemic circulation relatively rapidly.²¹⁻²³ Therefore, the i.p. administration of anticancer nanoparticles can effectively deliver the drugs into the peritoneal cavity, achieving a long retention time. The surface charge and size of the nanoparticles affect the i.p. retention time.^{24,25} The i.p. administration of cationic nanoparticles demonstrated a longer i.p. retention time than that of anionic nanoparticles because cationic nanoparticles bind electrostatically to the negatively charged peritoneum.²⁶ However, cationic nanoparticles strongly interact with biogenic substances, and this affects the distribution of the nanoparticles in the peritoneal cavity, depending on their modified physicochemical properties.²⁷ Furthermore, cationic

nanoparticles show potent cytotoxicity against not only cancer cells but also healthy cells.²⁸ Such undesirable effects hamper the use of cationic nanoparticles for the treatment of peritoneal dissemination. Compared with cationic nanoparticles, anionic nanoparticles show high biocompatibility without serious cytotoxicity due to less interaction with biogenic substances.²⁹ Moreover, anionic nanoparticles show high stability without any change in assembly and particle size even in biofluids such as ascites and blood²⁷; therefore they are expected to maintain their size while in the disease environment of the peritoneal cavity. Therefore, we hypothesized that i.p. administration of anionic nanoparticles containing anticancer agents that act specifically on cancer cells would be an effective therapy for peritoneal dissemination without side effects.

α -Tocopheryl succinate (TS), a succinic acid ester of α -tocopherol (α -T), is a redox-silent analog of α -T.³⁰ Although physiological actions of α -tocopherol and its analogs are based on their antioxidative effects,³⁰ TS exerts multifaceted anticancer effects such as the induction of cancer cell-specific apoptosis and inhibition of tumor angiogenesis and multidrug-resistant protein.³⁰ Because esterase activity of healthy cells is higher than that of cancer cells, TS is easily hydrolyzed to α -T, a silent agent with anticancer effects, leading to mitigation of undesirable side effects.³⁰ Alternatively, TS with both hydrophilic and hydrophobic moieties is easily vesiculated, while nanoparticles consisting only of TS undergo structural changes and disassemble in the presence of divalent cations and serum *in vivo*.³¹ We have previously developed nanoparticles (TS-NP) containing TS and egg phosphatidylcholine (EPC) to improve particle stability *in vivo*.³¹ TS-NP exhibited anionic surface charges and high particle stability *in vivo*,³¹ which is an advantageous physicochemical property for the treatment of peritoneal dissemination using i.p. administration of anticancer nanoparticles. When TS-NP were administered into tumor-bearing mice via the i.v. route, they existed as particles and were taken up by cancer cells at the tumor site, and they showed more potent anticancer effects than by TS itself.³¹ However, it was unclear whether TS-NP showed long retention in the peritoneal cavity and exerts potential antitumor effects when administered via the i.p. route in a mouse model of peritoneal dissemination.

In the present study, we compared the retention time of TS-NP in the peritoneal cavity after its i.v. and i.p. administration; moreover, multifaceted anticancer effects of TS-NP were determined in the mouse model of peritoneal dissemination. This mouse model was prepared by i.p. injection of colon26 (mouse colon cancer cell line) cells stably expressing the luciferase gene to monitor the growth of cancer cells. To analyze the i.p. retention time of nanoparticles and to determine the effect on particle size of nanoparticles, quantum dots (Qd) consisting of Cd/Se were encapsulated into TS-NP. Qd are nanoscale semiconductor crystals and highly biostable nanoparticles that have unique emission characteristics depending on the particle size and are widely used for biological imaging.³² Collectively, we demonstrated that TS-NP administered via the i.p. route were effectively retained in the peritoneal cavity, leading to potent anticancer effects, including diminished peritoneal dissemination and inhibition of ascites production.

2 | MATERIALS AND METHODS

2.1 | Reagents and materials

TS and EPC were purchased from Sigma Aldrich (St. Louis, MO, USA) and the NOF Corporation (Tokyo, Japan), respectively. 1,2-Dioleoyl-3-trimethylammonium propane (DOTAP) and 1,2-dioleoyl-sn-glycero-3-phosphoethanolamine-*N*-(lissamine rhodamine B sulfonyl) (Rh-PE) were purchased from Avanti Polar Lipids (Alabaster, AL, USA). LysoTracker Green DND-26, Qdot 705 ITK carboxyl quantum dots (Carboxyl-Qd), and Alexa488-labeled anti-rabbit antibody were purchased from Thermo Fisher Scientific Inc. (Waltham, MA, USA). Rabbit anti-CD163 antibody was purchased from Bioss Inc. (Woburn, MA, USA). VivoGlo™ Luciferin and Premix WST-1 Cell Proliferation Assay System were obtained from Promega (Madison, WI, USA) and TaKaRa Bio Inc. (Kyoto, Japan), respectively. Stearylated octaarginine (STR-R8) was synthesized by Scrum Inc. (Tokyo, Japan). The mouse colon cancer cell line, colon26, was provided by the RIKEN BRC under the National Bio-Resource Project of the MEXT/AMED, Japan. Colon26 cells stably expressing the luciferase gene (colon26-Luc) were established in our laboratory. Male Hos:HR-1 hairless and BALB/cCrSlc mice were purchased from Shimizu Laboratory Supplies Co., Ltd. (Kyoto, Japan). All mice were maintained and used in accordance with the animal protocol approved by the Institutional Animal Care and Use Committee of Kyoto Pharmaceutical University (Kyoto, Japan).

2.2 | Preparation of nanoparticles containing TS (TS-NP and TS-NP-Qd)

TS-NP were prepared using a simple hydration method described in our previous study.³¹ Briefly, to form a thin film, TS (50 mM) and EPC (32 mM) dissolved in ethanol were mixed in a round-bottomed glass tube at a molar ratio of 5:3.2 and then dried using nitrogen gas. The thin film was hydrated with PBS (-) containing 40 mM NaOH, and then nanoparticles were formed by sonication for 20 min in a bath-type sonicator (Yamato Scientific Co., Ltd., Tokyo, Japan). To encapsulate Qd into the TS-NP, a cationic core was prepared using surface modification of carboxyl-Qd using STR-R8. The anionic thin film consisting of TS and EPC was hydrated using this cationic core solution, followed by sonication for 20 min in a bath-type sonicator (Yamato Scientific Co., Ltd.). The unencapsulated Qd was removed using Vivaspin 6 Centrifugal Concentrators (0.20 μm) (Vivaproducts, Inc., MA, USA). The fluorescence intensity of Qd encapsulated in TS-NP (TS-NP-Qd) was measured using Plate manager Infinite M200 (Tecan) at an excitation wavelength of 401 nm and an emission wavelength of 705 nm. The lipid concentration of TS-NP was determined using the Wako's Phospholipids C assay kit (FUJIFILM Wako Pure Chemical Corp. Oosaka, Japan). The particle size and surface charge of the nanoparticles were determined using Zetasizer Nano (Malvern Instruments Ltd, Worcestershire, UK).

2.3 | Stability of TS-NP in the presence of ascites

To obtain ascites, colon26 cells (2×10^5) suspended in PBS (-) were intraperitoneally (i.p.) administered to BALB/cCrSlc mice, followed by the collection of ascites at 2 weeks after the injection. The ascites sample at 4x dilution with PBS was incubated with TS-NP at room temperature for 0, 1, or 24 h. The change in particle size and surface charge indicated the stability of the TS-NP in the presence of ascites.

2.4 | Biodistribution of TS-NP-Qd in the mouse model of peritoneal dissemination by an in vivo imaging system (IVIS) and inductively coupled plasma mass spectrometry (ICP-MS)

The mouse model of peritoneal dissemination was prepared by i.p. injection of colon26-Luc cells into HR:Hos-1 mice (2×10^5 cells/mouse). After 11 days, VivoGlo Luciferin was i.p. administered 15 min before image acquisition, and luminescence images were acquired using the IVIS Lumina XR imaging system (PerkinElmer Inc., MA, USA) equipped with an open luminescence filter with an exposure time of 20 s. After measuring the luminescence intensity that indicated the formation of peritoneal dissemination, TS-NP-Qd and carboxyl-Qd were administered i.v. and i.p. at a dose equivalent to 50 pmol/mouse Cd. The Qd in the mice was visualized by IVIS at an excitation wavelength of 420 nm, an emission wavelength of 710 nm, and an exposure time of 10 s. For the quantification of Qd by ICP-MS, ascites, peritoneum, and blood samples were collected 18 h after the injection. These samples were freeze dried using a FD-1000 dehydrator (EYELA, Tokyo, Japan) and then heated repeatedly in 60 wt% HNO₃, 60 wt% HClO₄, and 30 wt% H₂O₂ at -140°C to obtain a white powder. The powder was dissolved in 5% HNO₃ and used as a sample for ICP-MS. The concentration of Cd in Qd was determined using Agilent 7700 ICP-MS spectrometer (Agilent Technologies, CA, USA).

2.5 | Evaluation of tumor growth in mice using luminescence images

Colon26-Luc cells were injected i.p. into BALB/cCrSlc mice as described above. TS-NP and TS in ethanol (TS solution) were administered i.p. to these mice, at a dose equivalent to 4 mg of TS, 5 and 8 days after inoculation. TS was dissolved in sesame oil to prepare the TS solution used in the animal studies. Luminescence images indicating tumor growth were acquired using an IVIS spectrum imaging system (PerkinElmer Inc.) equipped with an open luminescence filter with an exposure time of 120 s at 25 min after the subcutaneous administration of VivoGlo Luciferin, and the radiance (photons per second per cm² per steradian) of the region of interest (ROI) was quantified using Living Image software (PerkinElmer Inc.).³³

2.6 | Quantification of ascites production and VEGF-A, IL-10 and TNF- α levels in blood

TS-NP were administered i.p. to the mice at a dose equivalent to 2 mg of TS at 4 and 11 days after inoculation. The ascites and blood were collected at 18 days after inoculation. Vascular endothelial growth factor A (VEGF-A), interleukin 10 (IL-10), and tumor necrosis factor alpha (TNF- α) levels in blood were determined using the Mouse VEGF Quantikine ELISA kit (R&D Systems, Inc., MN, USA) and Mouse IL-10 ELISA Kit (ThermoFisher Scientific Inc. (IBM Corp., MA, USA), respectively.

2.7 | Determination of cell viability using WST-1 assay

A cell viability assay was performed as previously described.³¹ Colon26 cells were seeded on 96-well CellBIND plates (Corning) at a density of 5×10^3 cells/well. After incubation at 37°C for 24 h, the cells were treated with TS-NP or TS dissolved in ethanol (TS solution) for 48 h. Cell viability was determined using the WST-1 assay. Cell viability was estimated by dividing the absorbance (at 440 nm) of the sample by that of the nontreated group.

2.8 | Evaluation of the cellular uptake and intracellular trafficking of TS-NPs

The cellular uptake of nanoparticles was determined using flow cytometry, as previously described.³¹ Colon26 cells were treated with EPC/DOTAP (7:3) liposomes and TS-NPs containing 1 mol% Rh-PE for 2 h. After washing twice with PBS (-) containing 2% FBS, the resuspended cells were subjected to flow cytometry analysis. The intracellular trafficking of TS-NPs was evaluated using confocal laser scanning microscopy, as previously described.³¹ The cells were treated with Rh-PE-labeled TS-NP for 2 h. The endosomes/lysosomes and nuclei were stained with LysoTracker Green DND-26 and Hoechst 33342, respectively. The intracellular distribution of TS-NPs was observed using a Nikon AX confocal laser scanning microscope (Nikon Corporation, Tokyo, Japan).

2.9 | Determination of the type of TAM in ascites using flow cytometry

The ascites samples obtained (as described in Section 2.6.) were mixed with anti-CD163 antibody at 4°C for 1 h. After washing with PBS (-) containing 2% FBS, the samples were incubated with Alexa488-labeled anti-rabbit antibody at 4°C for 1 h. After washing with PBS (-) containing 2% FBS, CD163-positive macrophages were determined using flow cytometry.

TABLE 1 Physicochemical properties of TS-NP

	Particle size (nm) mean \pm SD (n = 3)	ζ -potential (mV) mean \pm SD (n = 3)	PDI
TS-NP	124 \pm 12	-39 \pm 8	0.345

Abbreviations: PDI, polydispersity index; TS-NP, tocopheryl succinate nanoparticles.

2.10 | Statistical analysis

Statistical significance was determined using Student's *t* test or one-way ANOVA, followed by Tukey's honest significant difference test. Statistical significance was set at $p < 0.05$.

3 | RESULTS

3.1 | Effect of TS-NP on colon cancer cell proliferation

The particle size and ζ -potential of TS-NP prepared in this study were estimated at ~ 120 nm and -40 mV, respectively (Table 1). It had been previously reported that TS-NP induced potent cell death in B16-F1 cells, a mouse melanoma cell line, due to their homogenous cellular uptake attributed to their high particle stability.³¹ To determine the potential application of TS-NP in the treatment of peritoneal dissemination derived from colon cancer cells, we determined the effect of TS-NP on the growth of colon26 cells. As shown in Figure 1B, TS-NP significantly inhibited cell proliferation in a dose-dependent manner. A cell viability assay of TS-NP and TS solution at concentrations equivalent to 50 μ M of TS was performed; TS-NP induced more potent cytotoxicity than TS solution in colon26 cells (Figure 1B). Because the mitochondria are reportedly an action site of TS, negatively charged TS-NP needs to be taken up by cells for the inhibition of cell proliferation.³⁴ In general, the cellular uptake of anionic nanoparticles is ineffective.³⁵ Therefore, we examined the cellular uptake of rhodamine-labeled TS-NPs in colon26 cells. As shown in Figure 1C, flow cytometric analysis revealed that the rhodamine-labeled TS-NPs were taken up by the colon26 cells, although the surface charge was negative. Furthermore, we examined the intracellular trafficking of rhodamine-labeled TS-NPs using confocal laser scanning microscopy. As shown in Figure 1D, red fluorescent signals were observed inside the cells without colocalization with endosome/lysosome markers. These results suggested that TS-NPs were taken up by colon26 cells and delivered into the cytoplasm, where mitochondria exist as an action site of TS, inhibiting the proliferation of colon26 cells.

3.2 | Stability of TS-NP in the presence of ascites

TS-NP showed high stability as particles in the presence of divalent cations and serum, reflecting the *in vivo* environment, and leading to

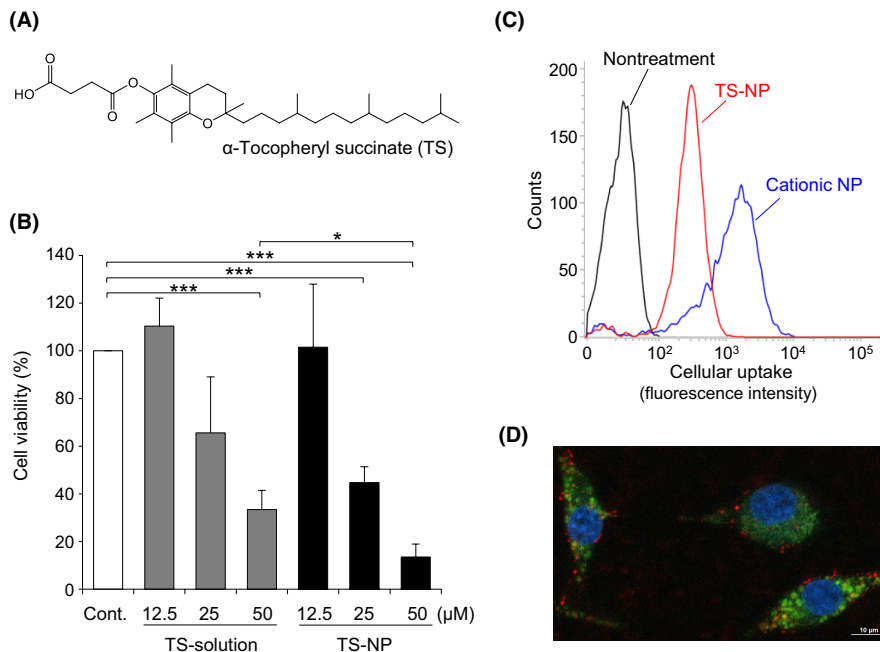
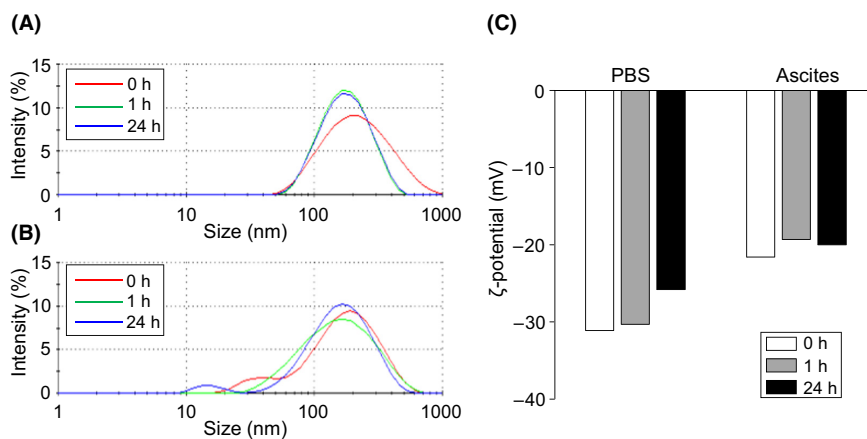


FIGURE 1 Effects of TS solution and TS-NP on colon-26 cell viability and the cellular uptake of TS-NP. (A) The chemical structure of tocopheryl succinate (TS). (B) Colon26 cells were treated with TS solution or TS-NP for 48 h. The cell viability was determined by the WST-1 assay. Values represent the means of three individual experiments. Bars represent standard deviation (SD). * $p < 0.05$ and *** $p < 0.001$. (C, D) Cellular uptake of TS-NP was determined by flow cytometry and confocal laser scanning microscopy (CLSM) 2 h after treatment with rhodamine-labeled nanoparticles. (C) Typical histograms of flow cytometric analysis. Black, red, and blue lines indicate nontreatment, TS-NP, and the cationic NP consisting of EPC and DOTAP (7:3), respectively. The cationic NP was used as a positive control. (D) A typical CLSM image showing the intracellular trafficking of TS-NP. Red, green, and blue signals indicate TS-NP, endosome/lysosome markers, and nuclei, respectively. TS solution, tocopheryl succinate dissolved in ethanol; TS-NP, tocopheryl succinate nanoparticles

FIGURE 2 Stability of TS-NP in the presence of ascites. (A, B) The distribution of particle size after incubation in PBS (-) (A) and in ascites (B). (C) Change in ζ -potential after incubation in PBS (-) and ascites. TS-NP, tocopheryl succinate nanoparticles



effective intratumoral distribution mediated using the EPR effect of negatively charged TS-NP.³¹ However, the stability of TS-NP in the abdominal cavity is unclear. Therefore, the physicochemical properties of TS-NP were evaluated in the presence of ascites. As shown in Figure 2A,C, the particle size distribution and ζ -potential of TS-NP in PBS were unchanged even after incubation for 24 h. The particle size in ascites showed a similar distribution to that in PBS, while smaller particles with size below 50 nm were observed (Figure 2B). As shown in Figure 2C, TS-NP has potent anionic charges even when incubated in ascites at 37°C for 24 h, although ζ -potential was

slightly attenuated from -30 to -20 mV after incubation. These results suggested the high stability of TS-NP in the presence of ascites.

3.3 | Biodistribution of i.p. and i.v. administration of TS-NP in mice

When nanoparticles are administered i.p., the biodistribution depends on their particle size.²¹⁻²³ To evaluate the biodistribution of TS-NP with a constant particle size, TS-NP-encapsulating

carboxyl-Qd was used in this study. To encapsulate negatively charged carboxyl-Qd in TS-NP, carboxyl-Qd was modified with positively charged STR-R8 (R8-Qd) (Figure 3A). The particle size and ζ -potential of R8-Qd were observed as 55 nm and +20 mV, respectively (Table 2). These positively charged R8-Qd were embedded into the negatively charged membranes of the TS-NP via electrostatic interaction (TS-NP-Qd) (Figure 3A). As shown in Table 2, the particle size of TS-NP-Qd was enlarged, and ζ -potential shifted from positive to negative compared with R8-Qd. These results confirmed the successful incorporation of carboxyl-Qd in TS-NP. The encapsulation efficiency of the Qds into the TS-NPs was $63 \pm 21\%$. The physicochemical properties of TS-NP-Qd in ascites were comparable with those in PBS, and were similar to TS-NP without cationic Qd cores, suggesting that TS-NP-Qd was also stable in ascites (Figure S1). Furthermore, using these TS-NP-Qd, the biodistribution of i.p. and i.v. administration of TS-NP was compared. TS-NP-Qd

injected i.p. were observed in the peritoneal cavity after 1 h of administration, whereas TS-NP-Qd injected i.v. were not (Figure 3B). When carboxyl-Qd was administered, weak signals were observed only for i.p. injection (Figure 3B). The retention time of TS-NP-Qd in the abdominal cavity was comparable with that of carboxyl-Qd, which was used as a control to evaluate the biodistribution of NPs with a constant particle size (Figure 3C). As shown in Figure 3C, the estimated half-life of TS-NP in the abdominal cavity was ~ 1 h. Consistent with the IVIS images, the amount of Qd in the ascites and peritoneum of mice after 18 h of i.p. injection of TS-NP-Qd was higher than that after i.v. injection (Figure 3D,E). As shown in Figure S2, the distribution of TS-NP-Qd in the liver, spleen, kidneys, and lungs 18 h after i.p. administration was similar to that after i.v. administration. These results suggested the potential delivery efficiency and retention of TS-NP-Qd after i.p. administration compared with i.v. administration.

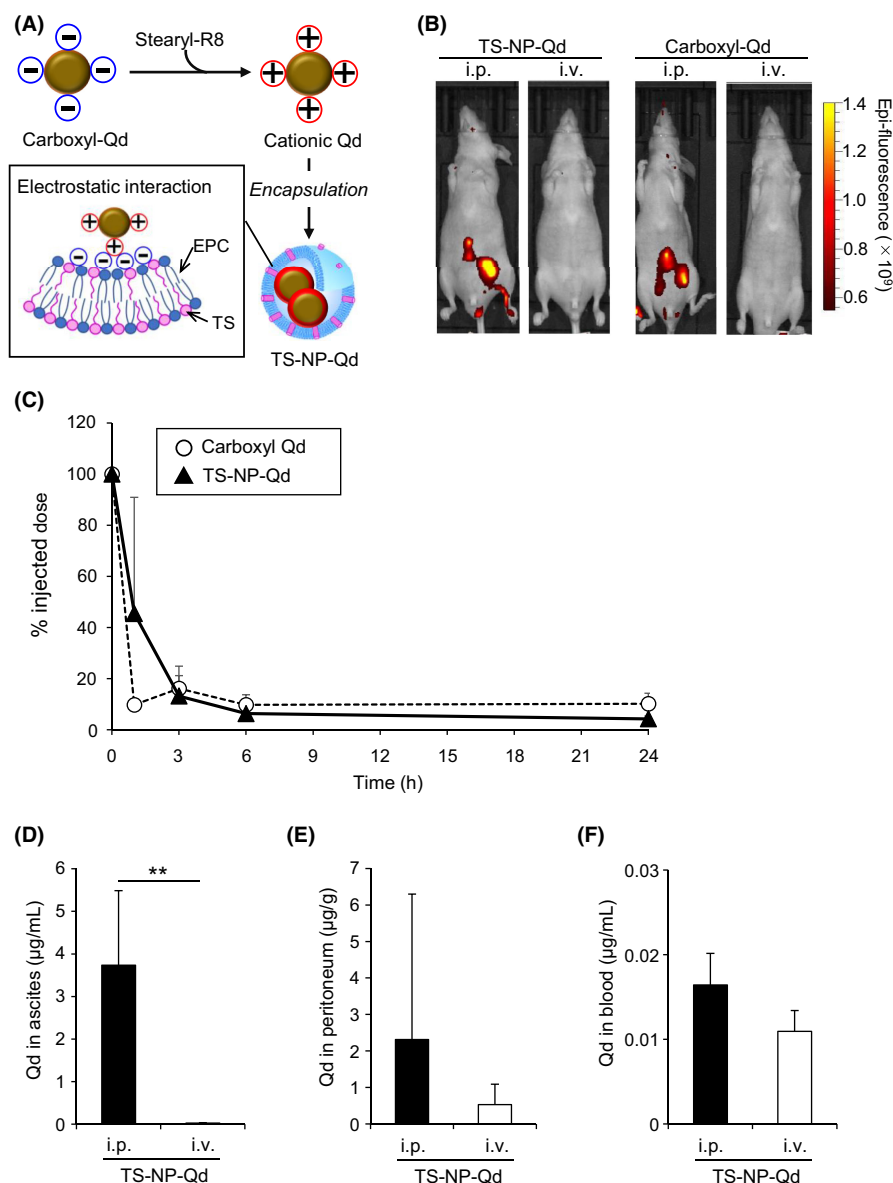


FIGURE 3 Biodistribution of TS-NP-Qd in peritoneal dissemination model mice. (A) Schematic diagram representing preparation of TS-NP-Qd. Negatively charged carboxyl-Qd was separated with positively charged stearyl-R8 to prepare cationic Qd. The cationic Qd was embedded into negatively charged TS-EPC membrane. The physicochemical properties of TS-NP-Qd are shown in Table 2. (B) Typical IVIS images of mice at 1 h after i.p. and i.v. administration of TS-NP-Qd or carboxyl-Qd. (C–F) The Qd levels were determined by ICP-MS. Values and bars represent the means and SD, respectively. (C) The Qd levels in ascites from mice 1, 3, 6, or 24 h after i.p. administration of TS-NP-Qd or carboxyl-Qd. Data are presented as a % of the injected dose. $n = 3$. (D–F) The Qd levels in ascites, peritoneum, and blood from mice at 18 h after i.p. and i.v. administration of TS-NP-Qd or carboxyl-Qd. The Qd levels were determined by ICP-MS. Values and bars represent means and SD, respectively. $n = 4$, $**p < 0.01$. i.p., intraperitoneal; i.v., intravenous; Qd, quantum dots; TS-NP-Qd, quantum dot encapsulated tocopheryl succinate nanoparticles; TS-EPC membrane, membrane consisting of tocopheryl succinate and egg phosphatidylcholine

3.4 | Inhibition of tumor growth by i.p. administered TS-NP in the mouse model of peritoneal dissemination

To determine the antitumor effect of TS-NP, colon26-Luc cells were inoculated into the peritoneal cavity, and then TS-NP and TS solution

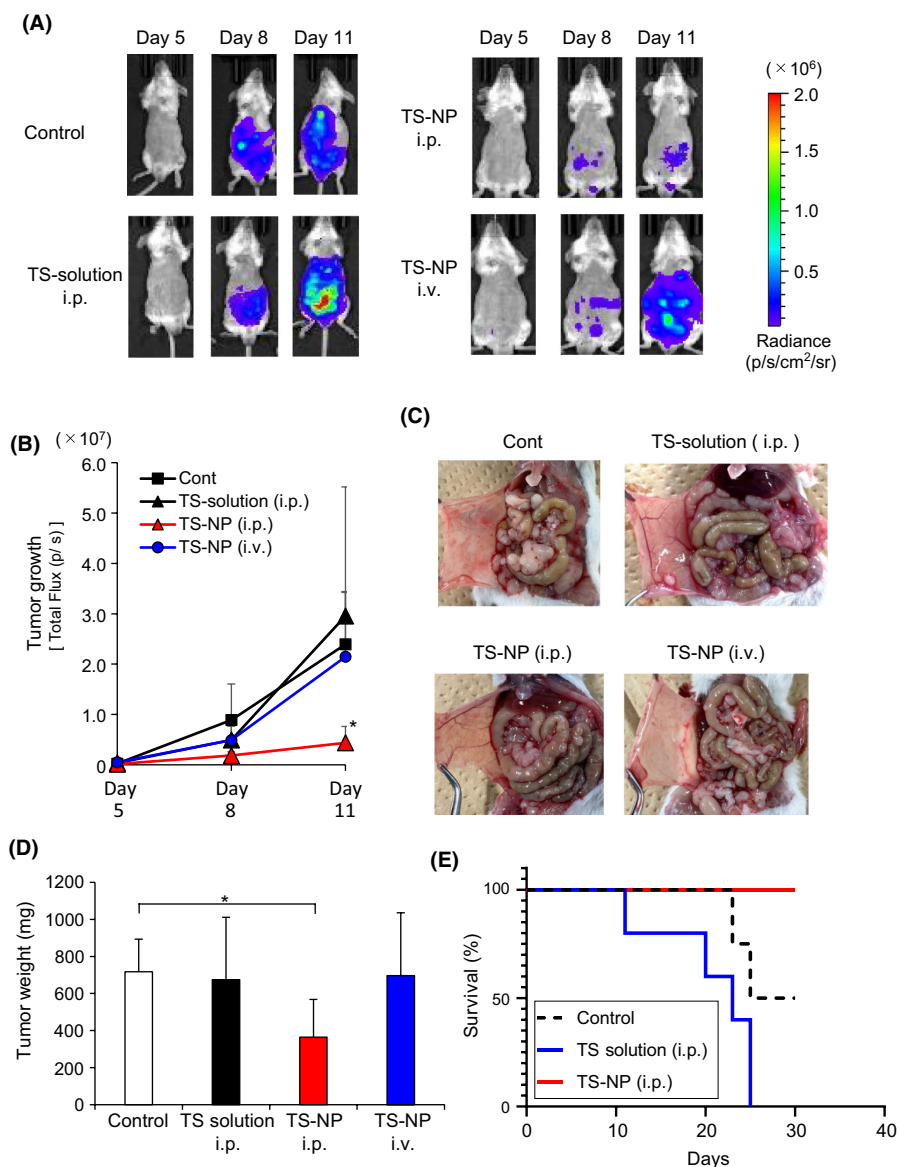
TABLE 2 Physicochemical properties of R8-Qd and TS-NP-Qd

	Particle size (nm)		PDI
	mean \pm SD (n = 3)	ζ -potential (mV) mean \pm SD (n = 3)	
R8-Qd	55 \pm 4	20 \pm 3	0.284
TS-NP-Qd	177 \pm 8	-25 \pm 0	0.457

Abbreviations: PDI, polydispersity index; R8-Qd, carboxyl-Qd modified with stearylated octaarginine; TS-NP, tocopheryl succinate nanoparticles; TS-NP-Qd, quantum dot encapsulated tocopheryl succinate nanoparticles.

FIGURE 4 Inhibition of tumor growth by intraperitoneally administered TS-NP. TS-NP and TS solution were intraperitoneally or intravenously administered to mice on day 5 and day 8. (A) Representative IVIS images of peritoneal dissemination model mice. Luminescence is derived from colon26 cells stably expressing luciferase gene. (B) Tumor growth in peritoneal dissemination model mice. Values and bars represent means and SD, respectively. $n = 3-5$, $*p < 0.05$. (C) Representative images of the peritoneum of mice receiving TS-NP or TS solution. (D) The weight of tumor nodules attached to the abdominal tissue of mice receiving TS-NP or TS solution. Values and bars represent means and SD, respectively. $n = 3-5$, $*p < 0.05$. (E) The survival periods of mice intraperitoneally administered TS solution or TS-NP. TS-NP, tocopheryl succinate nanoparticles; TS solution, TS dissolved in sesame oil; colon26, mouse colon cancer cell line

were administered i.p. or i.v. at 5 and 8 days after inoculation. IVIS images showed that the luminescence intensity indicating the number of living cancer cells decreased in TS-NP-administered mice compared with the control, TS-NP i.v.-injected mice, and TS solution i.p.-injected mice on day 11 (Figure 4A). The i.p. administration of TS-NP significantly inhibited tumor growth on day 11 after inoculation, whereas i.v. administration of TS-NP and i.p. administration of TS solution showed no effects (Figure 4B). Furthermore, the number of tumor nodules in the peritoneum of i.p.-administered TS-NP mice was lower than that in the peritoneum of the other groups (Figure 4C). The weight of the tumor nodules attached to abdominal tissue in the i.p.-administered TS-NP mice was also significantly lower than that in the control mice, whereas i.v. administration of TS-NP and i.p. administration of TS solution were ineffective (Figure 4D). Furthermore, the survival period of the i.p.-administered TS-NP mice was longer than that of control mice, while i.p. administration of TS solution was ineffective (Figure 4E). These results indicated that i.p. administration of TS-NP showed potent effects against peritoneal dissemination.



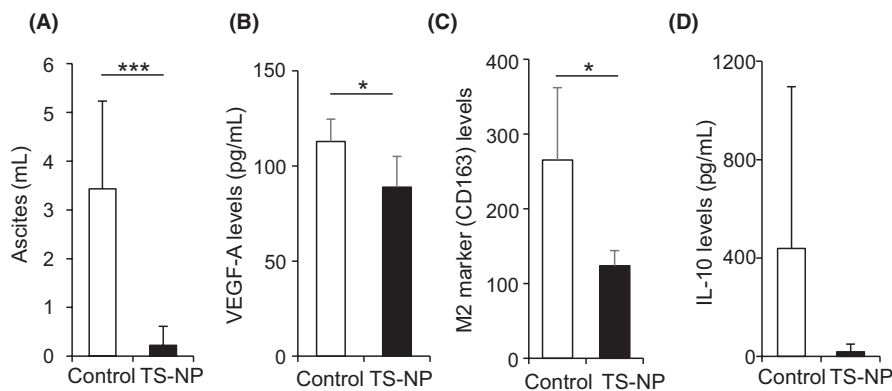


FIGURE 5 Improvement in intraperitoneal microenvironment by TS-NP. (A) The volume of ascites, (B, D) levels of VEGF-A and IL-10 and (C) CD163 levels as M2 marker in control and TS-NP administered mice. Values and bars represent means and SD, respectively. $n = 3-5$, $*p < 0.05$ and $***p < 0.001$. IL-10, interleukin 10; TS-NP, tocopheryl succinate nanoparticles; VEGF-A, vascular endothelial growth factor A

3.5 | Improvement in the i.p. microenvironment by TS-NP in the mouse model of peritoneal dissemination

We examined the effect of TS-NP on the i.p. microenvironment in the mouse model of peritoneal dissemination. As shown in Figure 5A, ascites production was significantly inhibited by the administration of TS-NP. Furthermore, the level of VEGF-A was significantly decreased (Figure 5B). It is known that vascular normalization and decreased ascites volume are attributed to improvement in the i.p. microenvironment, particularly the characteristic changes of TAM.³⁶ Because the M2-like phenotype of TAM contributes to tumor proliferation and progression,³⁷ we examined the amount of M2-like phenotype of TAM in ascites. As shown in Figure 5C, the level of CD163, which is an M2-like phenotype of the TAM marker,³⁸ significantly decreased in the ascites of TS-NP-administered mice. Furthermore, the level of IL-10, which activates M2-like polarization of TAM,³⁹ in ascites was decreased, however, the difference was not statistically significant. These results suggested improvement in the i.p. microenvironment by TS-NP via decrease in ascites production, VEGF-A and IL-10 levels, and M2-like polarization of TAM.

4 | DISCUSSION

In the present study, we evaluated the antitumor effects and biodistribution of i.p. administered TS-NP in a mouse model of peritoneal dissemination.

As shown in Figure 1B, TS-NP induced more potent cytotoxicity than TS solution in colon26 cells. The differences in cytotoxic effects of TS-NP and TS solution in colon26 cells were similar to that in B16-F1 cells.³¹ TS induces cell death via the production of mitochondrial O_2^- after direct binding to the ubiquinone-binding sites in mitochondrial respiratory complex II.³⁴ Therefore, effective delivery of TS inside the cell is required to induce potent cell death. We have previously analyzed the cellular uptake of TS molecules in B16-F1 cells using HPLC.³¹ The amount of TS in cells treated with TS-NPs was ~40% lower than that in cells treated with TS solution. Therefore, TS-NP strongly induced apoptosis, despite the low amounts of TS in

the cells treated with TS-NP. TS-NP were effectively delivered inside B16-F1 cells via endocytosis-mediated cellular uptake followed by efficient endosomal escape.³¹ As shown in Figure 1C,D, TS-NP was taken up by colon26 cells and delivered into the cytoplasm, where mitochondria exist as an active site of TS. Such nanoparticle-specific cellular uptake may lead to enhanced cell death induced by TS-NP in colon26 cells, similar to the effect in B16-F1 cells, although further mechanistic analysis is required. Therefore, TS-NP are expected to be a potential nanomedicine for colon cancer.

As shown in Figure 2, TS-NP showed high stability, even in the presence of ascites. Albumin is a major protein found in mouse peritoneal fluid, human ascites from patients with peritoneal carcinomatosis, and human serum from healthy donors.^{27,40} It has been considered that albumin, a negatively charged protein, barely interacts with negatively charged TS-NP, which was supported by unchanged particle size of TS-NP in the presence of 50% FBS.³¹ The stability of nanoparticles in body fluids depends on their surface charge.²⁷ In mice peritoneal fluid and human ascites, anionic nanoparticles showed high stability, whereas cationic nanoparticles strongly interacted with negatively charged proteins, such as albumin, due to their electrostatic interaction.²⁷ Therefore, negative surface charges on TS-NP contributed to their high stability in the presence of ascites.

As shown in Figure 3, i.p. administration of TS-NP-Qd showed potent i.p. delivery efficiency and retention in comparison with i.v. administration. The estimated half-life of TS-NPs in the abdominal cavity was ~1 h, as shown in Figure 3C. Furthermore, the retention time of TS-NP-Qd in the abdominal cavity was comparable with that of carboxyl-Qd with a particle size of ~20 nm. The i.p. retention time of the nanoparticles was affected by their particle size. Large-sized nanoparticles (>400 nm) remained in the peritoneal cavity for an extended duration.²³ Therefore, to extend the retention time of TS-NPs in the abdominal cavity, the physicochemical properties of TS-NPs must be improved by focusing on the particle size.

The i.p. administration of TS-NP showed a potent effect against peritoneal dissemination (Figure 4A-E). Although it was previously reported that i.p. administration of TS solution prevented liver metastasis of colon cancer,⁴¹ to the best of our knowledge, this is the first report indicating that the nanoparticles containing TS inhibit

the growth of colon cancer cells in the peritoneal cavity and peritoneum. As shown in Figure 3B–E, TS-NP showed efficient retention in the i.p. cavity that contributed to the potent antitumor effect. We previously reported that the antitumor effect of TS was not observed in half of the melanoma-bearing mice population receiving i.p. administration of TS solution.⁴² In tumor-bearing mice, antitumor effects were induced when TS molecules were translocated into the systemic blood circulation passing through the peritoneum. Conversely, the assembled TS molecules remained in the peritoneal cavity and were not effective. Alternatively, TS in the peritoneal cavity was not efficiently hydrolyzed to α -T due to low esterase activity in ascites.¹⁷ Therefore, the larger size of the TS-NP compared with that of the TS molecules led to effective i.p. retention, followed by induction of antitumor effects.

As shown in Figure 5A,B, i.p. administration of TS-NP inhibited ascites production and reduced VEGF-A levels. It is known that enhanced vascular permeability by angiogenesis-related factors, such as VEGF-A and angiopoietin-2 (Ang2), is one of the causes of ascites retention.^{43,44} TS suppresses VEGF-A and Ang2.⁴⁴ Ang2 acts on Tie2, an angiopoietin receptor, to destabilize the vascular structure by attenuating the interaction between endothelial cells and pericytes, followed by enhanced vascular permeability.⁴⁵ Although further studies are needed, stabilization of vascular structure through suppression of Ang2 expression followed by normalization of vascular permeability is a possible mechanism underlying inhibition of ascites production by TS-NP.

In the ascites of mice administered TS-NP i.p., the M2-like phenotypes of TAM and IL-10 decreased (Figure 5C, D). It has been reported that the M2-like polarization of TAM is mediated by IL-10.³⁹ TS-NP might have inhibited the M2-like polarization of TAM by decreasing IL-10 levels. Therefore, improvement in the i.p. microenvironment, such as vascular normalization and M2-like nonpolarized TAM, led to inhibition of tumor growth and ascites production by i.p. administration of TS-NP.

In summary, i.p. administered TS-NP showed potent retention in the peritoneal cavity. Consistent with the effective biodistribution, TS-NP inhibited tumor growth and improved the i.p. microenvironment by inhibiting ascites and VEGF-A production and decreasing the M2-like phenotype of TAM. Therefore, i.p. administration of TS-NP, which has multifaceted antitumor effects, is expected as a rational therapy for peritoneal dissemination.

ACKNOWLEDGMENTS

This work was supported in part by JSPS KAKENHI (Grant Number 18H03540). We would like to thank Editage (www.editage.com) for English language editing and Prof. Hiroyuki Yasui and Dr. Yuki Naito for their technical support during this study.

CONFLICT OF INTEREST

The author declares no conflict of interest.

ORCID

Susumu Hama  <https://orcid.org/0000-0002-2989-6168>

REFERENCES

- Li Y, Cong H, Wang S, Yu B, Shen Y. Liposomes modified with bio-substances for cancer treatment. *Biomater Sci*. 2020;8:6442-6468.
- Alven S, Aderibigbe BA. The therapeutic efficacy of dendrimer and micelle formulations for breast cancer treatment. *Pharmaceutics*. 2020;12:1212. doi:10.3390/pharmaceutics12121212
- Bayón-Cordero L, Alkorta I, Arana L. Application of solid lipid nanoparticles to improve the efficiency of anticancer drugs. *Nanomaterials*. 2019;9:474. doi:10.3390/nano9030474
- Khalil IA, Younis MA, Kimura S, Harashima H. Lipid nanoparticles for cell-specific in vivo targeted delivery of nucleic acids. *Biol Pharm Bull*. 2020;43:584-595. doi:10.1248/bpb.b19-00743
- Barani M, Hosseinihah SM, Rahdar A, et al. Nanotechnology in bladder cancer: diagnosis and treatment. *Cancers*. 2021;13:2214. doi:10.3390/cancers13092214
- Wyrozumska P, Meissner J, Toporkiewicz M, et al. Liposome-coated lipoplex-based carrier for antisense oligonucleotides. *Cancer Biol Ther*. 2015;16:66-76. doi:10.4161/15384047.2014.987009
- Golombek SK, May JN, Theek B, et al. Tumor targeting via EPR: Strategies to enhance patient responses. *Adv Drug Deliv Rev*. 2018;130:17-38. doi:10.1016/j.addr.2018.07.007
- Sukhbaatar A, Sakamoto M, Mori S, Kodama T. Analysis of tumor vascularization in a mouse model of metastatic lung cancer. *Sci Rep*. 2019;9:16029.
- Liu X, Jiang J, Meng H. Transcytosis - An effective targeting strategy that is complementary to "EPR effect" for pancreatic cancer nano drug delivery. *Theranostics*. 2019;9:8018-8025. doi:10.7150/thno.38587
- Xie Y, Hang Y, Wang Y, et al. Stromal modulation and treatment of metastatic pancreatic cancer with local intraperitoneal triple miRNA/siRNA nanotherapy. *ACS Nano*. 2020;14:255-271. doi:10.1021/acsnano.9b03978
- Soma D, Kitayama J, Konno T, et al. Intraperitoneal administration of paclitaxel solubilized with poly (2-methacryloxyethyl phosphorylcholine-co n-butyl methacrylate) for peritoneal dissemination of gastric cancer. *Cancer Sci*. 2009;100:1979-1985. doi:10.1111/j.1349-7006.2009.01265.x
- Sun F, Feng M, Guan W. Mechanisms of peritoneal dissemination in gastric cancer. *Oncol Lett*. 2017;14:6991-6998. doi:10.3892/ol.2017.7149
- Lemoine L, Sugarbaker P, Van der Speeten K. Pathophysiology of colorectal peritoneal carcinomatosis: role of the peritoneum. *World J Gastroenterol*. 2016;22:7692-7707. doi:10.3748/wjg.v22.i34.7692
- Stukan M. Drainage of malignant ascites: patient selection and perspectives. *Cancer Manag Res*. 2017;9:115-130. doi:10.2147/CMAR.S100210
- Senger DR, Galli SJ, Dvorak AM, Perruzzi CA, Harvey VS, Dvorak HF. Tumor cells secrete a vascular permeability factor that promotes accumulation of ascites fluid. *Science*. 1983;219:983-985. doi:10.1126/science.6823562
- Nagy JA, Masse EM, Herzberg KT, et al. Pathogenesis of ascites tumor growth: vascular permeability factor, vascular hyperpermeability, and ascites fluid accumulation. *Cancer Res*. 1995;55:360-368.
- Shimada T, Nomura M, Yokogawa K, et al. Pharmacokinetic advantage of intraperitoneal injection of docetaxel in the treatment for peritoneal dissemination of cancer in mice. *J Pharm Pharmacol*. 2005;57:177-181. doi:10.1211/0022357055380
- Soma D, Kitayama J, Ishigami H, Kaisaki S, Nagawa H. Different tissue distribution of paclitaxel with intravenous and intraperitoneal administration. *J Surg Res*. 2009;155:142-146. doi:10.1016/j.jss.2008.06.049
- Coccolini F, Catena F, Glehen O, et al. Effect of intraperitoneal chemotherapy and peritoneal lavage in positive peritoneal cytology in gastric cancer. Systematic review and meta-analysis. *Eur J Surg Oncol*. 2016;42:1261-1267. doi:10.1016/j.ejso.2016.03.035

20. Dakwar GR, Shariati M, Willaert W, Ceelen W, De Smedt SC, Remaut K. Nanomedicine-based intraperitoneal therapy for the treatment of peritoneal carcinomatosis - Mission possible? *Adv Drug Deliv Rev*. 2017;108:13-24. doi:[10.1016/j.addr.2016.07.001](https://doi.org/10.1016/j.addr.2016.07.001)
21. Sadzuka Y, Hirota S, Sonobe T. Intraperitoneal administration of doxorubicin encapsulating liposomes against peritoneal dissemination. *Toxicol Lett*. 2000;116:51-59. doi:[10.1016/S0378-4274\(00\)00201-0](https://doi.org/10.1016/S0378-4274(00)00201-0)
22. Tsai M, Lu Z, Wang J, Yeh TK, Wientjes MG, Au JL. Effects of carrier on disposition and antitumor activity of intraperitoneal Paclitaxel. *Pharm Res*. 2007;24:1691-1701
23. Mirahmadi N, Babaei MH, Vali AM, Dadashzadeh S. Effect of liposome size on peritoneal retention and organ distribution after intraperitoneal injection in mice. *Int J Pharm*. 2010;383:7-13. doi:[10.1016/j.ijpharm.2009.08.034](https://doi.org/10.1016/j.ijpharm.2009.08.034)
24. Dadashzadeh S, Mirahmadi N, Babaei MH, Vali AM. Peritoneal retention of liposomes: effects of lipid composition, PEG coating and liposome charge. *J Control Release*. 2010;148:177-186. doi:[10.1016/j.jconrel.2010.08.026](https://doi.org/10.1016/j.jconrel.2010.08.026)
25. Alavi S, Haeri A, Mahlooji I, Dadashzadeh S. Tuning the physico-chemical characteristics of particle-based carriers for intraperitoneal local chemotherapy. *Pharm Res*. 2020;37:119.
26. Ohtsuka A, Murakami T. Anionic sites on the free surface of the peritoneal mesothelium: light and electron microscopic detection using cationic colloidal iron. *Arch Histol Cytol*. 1994;57:307-315. doi:[10.1679/aohc.57.307](https://doi.org/10.1679/aohc.57.307)
27. Dakwar GR, Zagato E, Delanghe J, et al. Colloidal stability of nano-sized particles in the peritoneal fluid: towards optimizing drug delivery systems for intraperitoneal therapy. *Acta Biomater*. 2014;10:2965-2975. doi:[10.1016/j.actbio.2014.03.012](https://doi.org/10.1016/j.actbio.2014.03.012)
28. Knudsen KB, Northeved H, Kumar PE, et al. In vivo toxicity of cationic micelles and liposomes. *Nanomedicine*. 2015;11:467-477. doi:[10.1016/j.nano.2014.08.004](https://doi.org/10.1016/j.nano.2014.08.004)
29. Xia T, Kovochich M, Brant J, et al. Comparison of the abilities of ambient and manufactured nanoparticles to induce cellular toxicity according to an oxidative stress paradigm. *Nano Lett*. 2006;6:1794-1807. doi:[10.1021/nl061025k](https://doi.org/10.1021/nl061025k)
30. Hama S, Kogure K. Nanoparticles consisting of tocopheryl succinate are a novel drug-delivery system with multifaceted antitumor activity. *Biol Pharm Bull*. 2014;37:196-200. doi:[10.1248/bpb.b13-00848](https://doi.org/10.1248/bpb.b13-00848)
31. Hama S, Utsumi S, Fukuda Y, et al. Development of a novel drug delivery system consisting of an antitumor agent tocopheryl succinate. *J Control Release*. 2012;161:843-851. doi:[10.1016/j.jconrel.2012.05.031](https://doi.org/10.1016/j.jconrel.2012.05.031)
32. Zheng W, Liu Y, West A, et al. Quantum dots encapsulated within phospholipid membranes: phase-dependent structure, photostability, and site-selective functionalization. *J Am Chem Soc*. 2014;136:1992-1999. doi:[10.1021/ja411339f](https://doi.org/10.1021/ja411339f)
33. Itakura S, Hama S, Matsui R, Kogure K. Effective cytoplasmic release of siRNA from liposomal carriers by controlling the electrostatic interaction of siRNA with a charge-invertible peptide, in response to cytoplasmic pH. *Nanoscale*. 2016;8:10649-10658. doi:[10.1039/C5NR08365F](https://doi.org/10.1039/C5NR08365F)
34. Dong LF, Low P, Dyason JC, et al. Alpha-tocopheryl succinate induces apoptosis by targeting ubiquinone-binding sites in mitochondrial respiratory complex II. *Oncogene*. 2008;27:4324-4335.
35. Miller CR, Bondurant B, McLean SD, et al. Liposome-cell interactions in vitro: effect of liposome surface charge on the binding and endocytosis of conventional and sterically stabilized liposomes. *Biochemistry*. 1998; 37:12875-12883. doi:[10.1021/bi980096y](https://doi.org/10.1021/bi980096y)
36. Moughon DL, He H, Schokrpur S, et al. Macrophage blockade using CSF1R inhibitors reverses the vascular leakage underlying malignant ascites in late-stage epithelial ovarian cancer. *Cancer Res*. 2015;75:4742-4752. doi:[10.1158/0008-5472.CAN-14-3373](https://doi.org/10.1158/0008-5472.CAN-14-3373)
37. Kuwada K, Kagawa S, Yoshida R, et al. The epithelial-to-mesenchymal transition induced by tumor-associated macrophages confers chemoresistance in peritoneally disseminated pancreatic cancer. *J Exp Clin Cancer Res*. 2018;37:307.
38. Reinartz S, Schumann T, Finkernagel F, et al. Mixed-polarization phenotype of ascites-associated macrophages in human ovarian carcinoma: correlation of CD163 expression, cytokine levels and early relapse. *Int J Cancer*. 2014;134:32-42. doi:[10.1002/ijc.28335](https://doi.org/10.1002/ijc.28335)
39. Liu Q, Yang C, Wang S, et al. Wnt5a-induced M2 polarization of tumor-associated macrophages via IL-10 promotes colorectal cancer progression. *Cell Commun Signal*. 2020;18:51.
40. Martel J, Young D, Young A, et al. Comprehensive proteomic analysis of mineral nanoparticles derived from human body fluids and analyzed by liquid chromatography-tandem mass spectrometry. *Anal Biochem*. 2011;418:111-125. doi:[10.1016/j.ab.2011.06.018](https://doi.org/10.1016/j.ab.2011.06.018)
41. Barnett KT, Fokum FD, Malafa MP. Vitamin E succinate inhibits colon cancer liver metastases. *J Surg Res*. 2002;106:292-298. doi:[10.1006/jsre.2002.6466](https://doi.org/10.1006/jsre.2002.6466)
42. Kogure K, Manabe S, Hama S, et al. Potentiation of anti-cancer effect by intravenous administration of vesiculated alpha-tocopheryl hemisuccinate on mouse melanoma in vivo. *Cancer Lett*. 2003;192:19-24. doi:[10.1016/S0304-3835\(02\)00683-3](https://doi.org/10.1016/S0304-3835(02)00683-3)
43. Melgar-Lesmes P, Tugues S, Ros J, et al. Vascular endothelial growth factor and angiotensin-2 play a major role in the pathogenesis of vascular leakage in cirrhotic rats. *Gut*. 2009;58:285-292. doi:[10.1136/gut.2008.155028](https://doi.org/10.1136/gut.2008.155028)
44. Hama S, Okamura Y, Kamei K, et al. α -Tocopheryl succinate stabilizes the structure of tumor vessels by inhibiting angiotensin-2 expression. *Biochem Biophys Res Commun*. 2020;521:947-951. doi:[10.1016/j.bbrc.2019.11.017](https://doi.org/10.1016/j.bbrc.2019.11.017)
45. Akwii RG, Sajib MS, Zahra FT, Mikelis CM. Role of angiotensin-2 in vascular physiology and pathophysiology. *Cells*. 2019;8:471. doi:[10.3390/cells8050471](https://doi.org/10.3390/cells8050471)

SUPPORTING INFORMATION

Additional supporting information may be found in the online version of the article at the publisher's website.

How to cite this article: Hama S, Nishi T, Isono E, et al. Intraperitoneal administration of nanoparticles containing tocopheryl succinate prevents peritoneal dissemination. *Cancer Sci*. 2022;113:1779-1788. doi:[10.1111/cas.15321](https://doi.org/10.1111/cas.15321)